JOURNAL OF THEORETICAL AND APPLIED MECHANICS
51, 4, pp. 1067-1079, Warsaw 2013

ELASTIC SOLUTION OF PRESSURIZED CLAMPED-CLAMPED THICK CYLINDRICAL SHELLS MADE OF FUNCTIONALLY GRADED MATERIALS

Mehdi Ghannad

Shahrood University of Technology, Mechanical Engineering Faculty, Shahrood, Iran

e-mail: mghannadk@shahroodut.ac.ir

Mohammad Zamani Nejad

Yasouj University, Mechanical Engineering Department, Yasouj, Iran

e-mail: m.zamani.n@gmail.com; m_zamani@mail.yu.ac.ir

The effect of material inhomogeneity on displacements and stresses of an internally pressurized clamped-clamped thick hollow cylinder made of functionally graded materials is investigated. The modulus of elasticity is graded along the radial direction according to power functions of the radial direction. It is assumed that Poisson's ratio is constant across the cylinder thickness. The governing differential equations were generally derived, making use of the first-order shear deformation theory (FSDT). Following that, the set of non-homogenous linear differential equations for the cylinder with clamped-clamped ends was solved, and the effect of loading and supports on the stresses and displacements was investigated. The problem was also solved, using the finite element method (FEM), the results of which were compared with those of the analytical method.

Key words: clamped-clamped thick cylinder, functionally graded material (FGM), shear deformation theory (SDT)

1. Introduction

From viewpoints of solid mechanics, functionally graded materials (FGMs) are non-homogeneous elastic mediums. Using this property in the FGMs, an engineer can design composite materials such that any portion of the materials reaches the same safety level. In the last two decades, FGMs have been widely used in engineering applications, particularly in high-temperature environment, microelectronic, power transmission equipment, etc. On the other hand, the thick cylinder is a pressure vessel commonly used in industry. From the strength analysis, it is seen that the most dangerous point is located at the inner portion of the cylinder, if homogeneous materials are used. However, if one uses the FMGs for a thick cylinder, this situation can be changed. Due to the importance of structural integrity, the safe design of such hollow cylindrical structures, in particular for functionally graded hollow annuli or tubes have attracted considerable attention in recent years. Naghdi and Cooper (1956), assuming the cross shear effect, formulated the shear deformation theory (SDT). Mirsky and Hermann (1958), derived the solution of thick cylindrical shells of homogenous and isotropic materials, using the first shear deformation theory (FSDT). Using the shear deformation theory and Frobenius series, Suzuki *et al.* (1981), obtained the solution of the free vibration of cylindrical shells with variable thickness. Kang (2007) derived the field equations for homogenous thick shells of revolution. Eipakchi *et al.* (2003) obtained the solution of the homogenous and isotropic thick-walled cylindrical shells with variable thickness, using the first-order shear deformation theory (FSDT) and the perturbation technique. Hongjun *et al.* (2006), and Zhifei *et al.* (2007), provided elastic analysis and the exact solution for stresses in FGM hollow cylinders in the state of plane strain

with isotropic multi-layers based on Lamé's solution. Nejad and Rahimi (2010), obtained stresses in isotropic rotating thick-walled cylindrical pressure vessels made of a functionally graded material as a function of the radial direction by using the theory of elasticity. Pan and Roy (2006) derived exact solutions for multilayered FGM cylinders under static deformation. They obtained these solutions by making use of the method of separation of variables and expressed it in terms of the summation of the Fourier series in the circumferential direction. A complete and consistent 3D set of field equations was developed by tensor analysis to characterize the behavior of FGM thick shells of revolution with arbitrary curvature and variable thickness along the meridional direction by Nejad *et al.* (2009). Using plane elasticity theory and Complementary Functions method, Tutuncu and Temel (2009) obtained axisymmetric displacements and stresses in functionally-graded hollow cylinders, disks and spheres subjected to uniform internal pressure. Assuming that the shear modulus varies in the radial direction either according to a power law relation or an exponential function, Batra and Nie (2010) obtained analytically plane strain infinitesimal deformations of a non-axisymmetrically loaded hollow cylinder and of an eccentric cylinder composed of a linear elastic isotropic and incompressible functionally graded material. Using the Airy stress function, Nie and Batra (2010) presented exact solutions for plane strain deformations of a functionally graded hollow cylinder with the inner and the outer surfaces subjected to different boundary conditions. Making use of FSDT and the virtual work principle, Ghannad and Nejad (2010) generally derived the differential equations governing the homogenous and isotropic axisymmetric thick-walled cylinders with the same boundary conditions at the two ends. Following that, the set of nonhomogenous linear differential equations for the cylinder with clamped-clamped ends was solved. Ghannad *et al.* (2012) also obtained the general solution of the clamped-clamped thick cylindrical shells with variable thickness subjected to constant internal pressure using the first shear deformation theory. Ostrowski and Michalak (2011) investigated the effect of geometry and material properties on the temperature field in a two-phase hollow cylinder.

In this paper, taking into account the effect of shear stresses and strains, the general method of derivation and the analysis of an internally pressurized thick-walled cylinder shell made of a functionally graded material with clamped-clamped ends are presented.

2. Problem formulation

Consider a clamped-clamped thick-walled isotropic FGM cylinder with an inner radius r_i, thickness h, and length L subjected to internal pressures P.

Given that the radial coordinate r is normalized as $\overline{r} = r/r_i$. The modulus of elasticity E is assumed to be radially dependent and is assumed to vary as follows

$$E(r) = E_i(\overline{r})^n = \frac{E_i}{r_i^n} r^n \tag{2.1}$$

Here E_i is the modulus of elasticity at the inner surface r_i and n is the inhomogeneity constant determined empirically. Since the analysis was done for a thick wall cylindrical pressure vessel of an isotropic FGM, and given that the variation of Poisson's ratio ν for engineering materials is small, it is assumed as constant.

The range $-1 \leqslant n \leqslant +1$ to be used in the present study covers all the values of coordinate exponent encountered in the references cited earlier. However, these values for n do not necessarily represent a certain material.

The plane elasticity theory (PET) or classical theory is based on the assumption that the straight lines perpendicular to the central axis of the cylinder remain unchanged after loading and deformation. According to this theory, the deformations are axisymmetric and do not change

along the longitudinal cylinder. In other words, the elements do not have any rotation, and the shear strain is assumed to be zero

$$\begin{aligned} &u_r = u_r(r) \qquad\qquad u_x = u_x(x) \\ &\gamma_{rx} = \frac{\partial u_r}{\partial x} + \frac{\partial u_x}{\partial r} = 0 \;\Rightarrow\; \tau_{rx} = 0 \end{aligned} \tag{2.2}$$

Therefore, equilibrium equations are independent of one another, and the coupling of the equations is deleted

$$\frac{d\sigma_r}{dr} + \frac{1}{r}(\sigma_r - \sigma_\theta) = 0 \qquad\qquad \frac{d\sigma_x}{dx} = 0 \tag{2.3}$$

The differential equation based on the Navier solution in terms of the radial displacement is (Ghannad *et al.*, 2010)

$$r^2\frac{d^2u_r}{dr^2} + (n+1)r\frac{du_r}{dr} + (n\nu^* - 1)u_r = 0 \tag{2.4}$$

ν^* is defined based on boundary conditions. The solution to the Eq. (2.4) based on real roots is as follows

$$u_r(r) = C_1 r^{m_1} + C_2 r^{m_2} \qquad\qquad m_{1,2} = \frac{1}{2}\Big[-n \pm \sqrt{n^2 - 4(n\nu^* - 1)}\Big] \tag{2.5}$$

This method is applicable to problems in which the shear stress τ_{rx} and shear strain γ_{rx}, are considered zero. However, to solve the problems such as the following, it is not possible to use the PET

$$\begin{aligned} &u_r = u_r(x,z) \qquad\qquad u_x = u_x(x,z) \\ &\gamma_{rx} = \frac{\partial u_r}{\partial x} + \frac{\partial u_x}{\partial r} \neq 0 \quad\Rightarrow\quad \tau_{rx} \neq 0 \end{aligned} \tag{2.6}$$

In the shear deformation theory (SDT), the straight lines perpendicular to the central axis of the cylinder do not necessarily remain unchanged after loading and deformation, suggesting that the deformations are axial axisymmetric and change along the longitudinal cylinder. In other words, the elements have rotation, and the shear strain is not zero.

In Fig. 1, the location of a typical point m, r, within the shell element may be determined by R and z, as

$$r = R + z \tag{2.7}$$

where R represents the distance of the middle surface from the axial direction, and z is the distance of a typical point from the middle surface.

In Eq. (2.7), x and z must be as follows

$$-\frac{h}{2} \leqslant z \leqslant \frac{h}{2} \qquad\qquad 0 \leqslant x \leqslant L \tag{2.8}$$

where h and L are the thickness and the length of the cylinder.

The general axisymmetric displacement field (U_x, U_z) in the first-order shear deformation theory could be expressed on the basis of axial and radial displacements, as follows (Mirsky and Hermann, 1958)

$$\begin{Bmatrix} U_x \\ U_z \end{Bmatrix} = \begin{Bmatrix} u(x) \\ w(x) \end{Bmatrix} + \begin{Bmatrix} \phi(x) \\ \psi(x) \end{Bmatrix} z \tag{2.9}$$

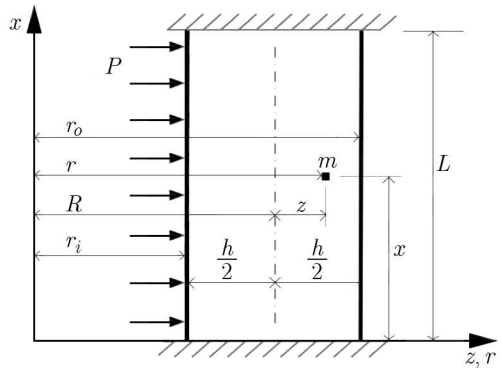

Fig. 1. Cross section of the thick cylinder with clamped-clamped ends

where $u(x)$ and $w(x)$ are the displacement components of the middle surface. Also, $\phi(x)$ and $\psi(x)$ are functions of the displacement field.

The strain-displacement relations in the cylindrical coordinates system are

$$\begin{aligned} \varepsilon_x &= \frac{\partial U_x}{\partial x} = \frac{du}{dx} + \frac{d\phi}{dx}z \qquad & \varepsilon_\theta &= \frac{U_z}{r} = \frac{1}{R+z}(w + \psi z) \\ \varepsilon_z &= \frac{\partial U_z}{\partial z} = \psi & \gamma_{xz} &= \frac{\partial U_x}{\partial z} + \frac{\partial U_z}{\partial x} = \Big(\phi + \frac{dw}{dx}\Big) + \frac{d\psi}{dx}z \end{aligned} \tag{2.10}$$

The distribution of elasticity modulus basis on Eq. (2.1) and Eq. (2.7) is

$$E(r) = E_i\Big(\frac{R+z}{r_i}\Big)^n = \frac{E_i}{r_i^n}(R+z)^n = E(z) \tag{2.11}$$

The stresses on the basis of constitutive equations for homogenous and isotropic materials are as follows

$$\begin{aligned} \sigma_i &= \lambda E(z)[(1-\nu)\varepsilon_i + \nu(\varepsilon_j + \varepsilon_k)] \qquad & i \neq j \neq k \\ \tau_{xz} &= \lambda E(z)\Big[(1-2\nu)\frac{\gamma_{xz}}{2}\Big] \qquad & \lambda = \frac{1}{(1+\nu)(1-2\nu)} \end{aligned} \tag{2.12}$$

where σ_i and ε_i are the stresses and strains in the axial x, circumferential θ, and radial z directions, respectively.

The normal forces N_x, N_θ, N_z, shear force Q_x, bending moments M_x, M_θ, M_z, and the torsional moment M_{xz} in terms of stress resultants are

$$\begin{aligned} \{N_x, N_\theta, N_z\} &= \int_{-h/2}^{h/2} \Big[\sigma_x\Big(1+\frac{z}{R}\Big), \sigma_\theta, \sigma_z\Big(1+\frac{z}{R}\Big)\Big]\, dz \\ \{M_x, M_\theta, M_z\} &= \int_{-h/2}^{h/2} \Big[\sigma_x\Big(1+\frac{z}{R}\Big), \sigma_\theta, \sigma_z\Big(1+\frac{z}{R}\Big)\Big] z\, dz \\ Q_x &= \int_{-h/2}^{h/2} \tau_{xz}\Big(1+\frac{z}{R}\Big)\, dz \qquad M_{xz} = \int_{-h/2}^{h/2} \tau_{xz}\Big(1+\frac{z}{R}\Big) z\, dz \end{aligned} \tag{2.13}$$

On the basis of the principle of virtual work, the variations of strain energy are equal to the variations of the external work as follows

$$\delta U = \delta W \tag{2.14}$$

where U is the total strain energy of the elastic body and W is the total external work due to internal pressure. The strain energy is

$$\begin{aligned} U &= \iiint_V U^* \, dV \qquad\qquad dV = r \, dr \, d\theta \, dx = (R+z) \, dx \, d\theta \, dz \\ U^* &= \frac{1}{2}(\sigma_x \varepsilon_x + \sigma_\theta \varepsilon_\theta + \sigma_z \varepsilon_z + \tau_{xz}\gamma_{xz}) \end{aligned} \tag{2.15}$$

and the external work is

$$W = \iint_S (\mathbf{f} \cdot \mathbf{u}) \, dS \qquad dS = r_i \, d\theta \, dx = \Big(R - \frac{h}{2}\Big) \, d\theta \, dx \qquad \mathbf{f} \cdot \mathbf{u} = PU_z \tag{2.16}$$

The variation of the strain energy is

$$\delta U = R \int_0^{2\pi} \int_0^L \int_{-h/2}^{h/2} \delta U^* \Big(1 + \frac{z}{R}\Big)) \, dz \, dx \, d\theta \tag{2.17}$$

Resulting Eq. (2.17) will be

$$\frac{\delta U}{2\pi} = R \int_0^L \int_{-h/2}^{h/2} (\sigma_x \delta\varepsilon_x + \sigma_\theta \delta\varepsilon_\theta + \sigma_z \delta\varepsilon_z + \tau_{xz}\delta\gamma_{xz}) \Big(1 + \frac{z}{R}\Big) \, dz \, dx \tag{2.18}$$

and the variation of the external work is

$$\delta W = \int_0^{2\pi} \int_0^L P \delta U_z \Big(R - \frac{h}{2}\Big) \, dx \, d\theta \tag{2.19}$$

Resulting Eq. (2.19) will be

$$\frac{\delta W}{2\pi} = P \int_0^L \delta U_z \Big(R - \frac{h}{2}\Big) \, dx \tag{2.20}$$

Substituting Eqs. (2.10) and (2.12) into Eq. (2.14), and drawing upon calculus of variation and the virtual work principle, we will have

$$\begin{aligned} R\frac{dN_x}{dx} &= 0 & R\frac{dM_x}{dx} - RQ_x &= 0 \\ R\frac{dQ_x}{dx} - N_\theta &= -P\Big(R - \tfrac{h}{2}\Big) & R\frac{dM_{xz}}{dx} - M_\theta - RN_z &= P\frac{h}{2}\Big(R - \frac{h}{2}\Big) \end{aligned} \tag{2.21}$$

and the boundary conditions at the two ends of cylinder are

$$R\Big[N_x \delta u + M_x \delta\phi + Q_x \delta w + M_{xz} \delta\psi\Big]_0^L = 0 \tag{2.22}$$

In order to solve the set of differential equations (2.21), forces and moments need to be expressed in terms of the components of the displacement field, using Eqs. (2.13). Thus, set of differential equations (2.21) could be derived as follows

$$\overline{\mathbf{A}}_1 \frac{d^2}{dx^2}\overline{\mathbf{y}} + \overline{\mathbf{A}}_2 \frac{d}{dx}\overline{\mathbf{y}} + \overline{\mathbf{A}}_3 \overline{\mathbf{y}} = \overline{\mathbf{F}} \qquad \overline{\mathbf{y}} = [u, \phi, w, \psi]^{\mathrm{T}} \tag{2.23}$$

The set of equations (2.23) is a set of linear non-homogenous equations with constant coefficients. $\overline{\mathbf{A}}_3$ is irreversible and its reverse is needed in the next calculations. In order to make $\overline{\mathbf{A}}_3^{-1}$, the first equation in the set of Eqs. (2.21) is integrated

$$RN_x = C_0 \tag{2.24}$$

In Eq. (2.23), it is apparent that u does not exist, but du/dx does. Taking du/dx as v

$$u = \int v\, dx + C_7 \tag{2.25}$$

Thus, set of differential equations (2.23) could be derived as follows:

$$\mathbf{A}_1 \frac{d^2}{dx^2}\mathbf{y} + \mathbf{A}_2 \frac{d}{dx}\mathbf{y} + \mathbf{A}_3\mathbf{y} = \mathbf{F} \qquad \mathbf{y} = [v, \phi, w, \psi]^{\mathrm{T}} \tag{2.26}$$

The set of equations (2.26) is a set of linear non-homogenous equations with constant coefficients.

3. Analytical solution

Defining the differential operator $P(D)$, Eq. (2.26) is written as

$$P(D) = \mathbf{A}_1 D^2 + \mathbf{A}_2 D + \mathbf{A}_3 \qquad D = \frac{d}{dx} \qquad D^2 = \frac{d^2}{dx^2} \tag{3.1}$$

Thus

$$P(D)\mathbf{y} = \mathbf{F} \tag{3.2}$$

Differential Eq. (3.2) has a general solution $\mathbf{y}_g$ and particular solution $\mathbf{y}_p$, as follows

$$\mathbf{y} = \mathbf{y}_g + \mathbf{y}_p \tag{3.3}$$

For the general solution, $\mathbf{y}_g = \mathbf{V}\mathrm{e}^{mx}$ is substituted in homogeneous Eq. (3.2)

$$\mathrm{e}^{mx}(m^2\mathbf{A}_1 + m\mathbf{A}_2 + \mathbf{A}_3)\mathbf{V} = \mathbf{0} \tag{3.4}$$

Given that $\mathrm{e}^{mx} \neq 0$, the following eigenvalue problem is created

$$(m^2\mathbf{A}_1 + m\mathbf{A}_2 + \mathbf{A}_3)\mathbf{V} = \mathbf{0} \tag{3.5}$$

To obtain the eigenvalues, the determinant of coefficients must be considered zero

$$\left|m^2\mathbf{A}_1 + m\mathbf{A}_2 + \mathbf{A}_3\right| = 0 \tag{3.6}$$

The result of the determinant above is a six-order polynomial which is a function of m, the solution of which is 6 eigenvalues m_i. The eigenvalues are 3 pairs of conjugated roots. Substituting the calculated eigenvalues into Eq. (3.5), the corresponding eigenvectors $\mathbf{V}_i$ are obtained. Therefore, the general solution for homogeneous Eq. (3.2) is

$$\mathbf{y}_g = \sum_{i=1}^{6} C_i \mathbf{V}_i \mathrm{e}^{m_i x} \tag{3.7}$$

Given that $\mathbf{F}$ is comprised of constant parameters, the particular solution is obtained as follows

$$\mathbf{y}_p = \mathbf{A}_3^{-1}\mathbf{F} \tag{3.8}$$

Therefore, the total solution for Eq. (3.2) is

$$\mathbf{y} = \sum_{i=1}^{6} C_i \mathbf{V}_i \mathrm{e}^{m_i x} + \mathbf{A}_3^{-1}\mathbf{F} \tag{3.9}$$

In total, the problem consists of 8 unknown values of C_i, including C_0 (Eq. (2.24)), C_1 to C_6 (Eq. (3.9)), and C_7 (Eq. (2.25)). By applying boundary conditions, one can obtain the constants of C_i. Given that the two ends of the cylinder are clamped-clamped, then

$$\begin{Bmatrix} u \\ \phi \\ w \\ \psi \end{Bmatrix}_{x=0} = \begin{Bmatrix} u \\ \phi \\ w \\ \psi \end{Bmatrix}_{x=L} = \begin{Bmatrix} 0 \\ 0 \\ 0 \\ 0 \end{Bmatrix} \tag{3.10}$$

4. Solution of FGM cylinders

In order to analyze FGM cylinders, substituting Eq. (2.11) into Eqs. (2.12) and then by using Eq. (2.10), the stress resultants in terms of the displacement field are obtained. With substituting stress resultants into Eqs (2.21), a set of nonhomogeneous differential equations with variable coefficients is obtained. The constants used are as follows

$$k = \frac{r_o}{r_i} \qquad \alpha = \ln k \qquad \beta = \frac{k-1}{k r_i} \qquad \mu = K\Big(\frac{1-2\nu}{2}\Big) \tag{4.1}$$

where K is the shear correction factor.

4.1. Inhomogeneity constant of $n = -1$

Based on Eq. (2.11), the modulus of elasticity is

$$E(z) = \frac{E_i r_i}{R+z} \tag{4.2}$$

The coefficients matrices $[\mathbf{A_i}]]_{4\times4}$ and the force vector $\mathbf{F}$ in Eq. (2.26) are

$$\begin{aligned}
\mathbf{A}_1 &= \begin{bmatrix} 0 & 0 & 0 & 0 \\ 0 & (1-\nu)\frac{h^3}{12} & 0 & 0 \\ 0 & 0 & \mu h & 0 \\ 0 & 0 & 0 & \mu\frac{h^3}{12} \end{bmatrix} \\
\mathbf{A}_2 &= \begin{bmatrix} 0 & 0 & 0 & 0 \\ 0 & 0 & \nu(h-R\alpha)-\mu h & \nu(R^2\alpha - Rh) \\ 0 & -\nu(h-R\alpha)+\mu h & 0 & 0 \\ 0 & -\nu(R^2\alpha - Rh) & 0 & 0 \end{bmatrix} \\
\mathbf{A}_3 &= \begin{bmatrix} (1-\nu)h & 0 & \nu\alpha & \nu(2h-R\alpha) \\ 0 & -\mu h & 0 & 0 \\ -\nu\alpha & 0 & -(1-\nu)\beta & -\alpha+(1+\nu)R\beta \\ -\nu(2h-R\alpha) & 0 & -\alpha+(1-\nu)R\beta & 2(R\alpha-h)-(1-\nu)R^2\beta \end{bmatrix} \\
\mathbf{F} &= \frac{1}{\lambda E_i r_i}\Big[C_0, 0, -P\Big(R-\frac{h}{2}\Big), P\frac{h}{2}\Big(R-\frac{h}{2}\Big)\Big]^{\mathrm{T}}
\end{aligned} \tag{4.3}$$

To obtain the eigenvalues m_i, the determinant of coefficients (Eq. (3.6)) must be considered zero

$$\begin{vmatrix} (1-\nu)h & 0 & \nu\alpha & \nu(2h-R\alpha) \\ 0 & m^2(1-\nu)\frac{h^3}{12}-\mu h & m\nu(h-R\alpha)-m\mu h & m\nu(R^2\alpha-Rh) \\ -\nu\alpha & -m\nu(h-R\alpha)+m\mu h & m^2\mu h-(1-\nu)\beta & -\alpha+(1+\nu)R\beta \\ -\nu(2h-R\alpha) & -m\nu(R^2\alpha-Rh) & -\alpha+(1-\nu)R\beta & b_{44} \end{vmatrix} = 0 \tag{4.4}$$

where

$$b_{44} = m^2\mu\frac{h^3}{12} + 2(R\alpha - h) - (1-\nu)R^2\beta$$

With solving of the obtained polynomial of the above determinant, the eigenvalues m_i and the following eigenvectors $\mathbf{V}_i$ are calculated. Finally, the total solution (Eq. (3.9)), with using boundary conditions is obtained.

4.2. Inhomogeneity constant of $n = +1$

Based on Eq. (2.11), the modulus of elasticity is

$$E(z) = \frac{E_i}{r_i}(R+z) \tag{4.5}$$

The coefficients matrices $[\mathbf{A}_i]_{4\times4}$, and force vector $\mathbf{F}$ in Eq. (2.26) are

$$\mathbf{A}_1 = \begin{bmatrix} 0 & 0 & 0 & 0 \\ 0 & (1-\nu)\Big(\frac{R^2h^3}{12}+\frac{h^5}{80}\Big) & 0 & 0 \\ 0 & 0 & \mu\Big(R^2h+\frac{h^3}{12}\Big) & \mu\frac{Rh^3}{6} \\ 0 & 0 & \mu\frac{Rh^3}{6} & \mu\Big(\frac{R^2h^3}{12}+\frac{h^5}{80}\Big) \end{bmatrix}$$

$$\mathbf{A}_2 = \begin{bmatrix} 0 & (1-\nu)\frac{Rh^3}{6} & 0 & 0 \\ (1-\nu)\frac{Rh^3}{6} & 0 & -\mu\Big(R^2h+\frac{h^3}{12}\Big)+\nu\frac{h^3}{12} & -(2\mu-3\nu)\frac{Rh^3}{12} \\ 0 & \mu\Big(R^2h+\frac{h^3}{12}\Big)-\nu\frac{h^3}{12} & 0 & 0 \\ 0 & (2\mu-3\nu)\frac{Rh^3}{12} & 0 & 0 \end{bmatrix} \tag{4.6}$$

$$\mathbf{A}_3 = \begin{bmatrix} (1-\nu)\Big(R^2h+\frac{h^3}{12}\Big) & 0 & \nu Rh & \nu\Big(R^2h+\frac{h^3}{6}\Big) \\ 0 & -\mu\Big(R^2h+\frac{h^3}{12}\Big) & 0 & 0 \\ -\nu Rh & 0 & -(1-\nu)h & -\nu Rh \\ -\nu\Big(R^2h+\frac{h^3}{6}\Big) & 0 & -\nu Rh & -(1-\nu)R^2h-\frac{h^3}{6} \end{bmatrix}$$

$$\mathbf{F} = \frac{r_i}{\lambda E_i}\Big[C_0, 0, -P\Big(R-\frac{h}{2}\Big), P\frac{h}{2}\Big(R-\frac{h}{2}\Big)\Big]^{\mathrm{T}}$$

To obtain the eigenvalues m_i, the determinant of coefficients (Eq. (3.6)) must be considered zero

$$\begin{vmatrix} c_{11} & m(1-\nu)\frac{Rh^3}{6} & \nu Rh & \nu\Big(R^2h+\frac{h^3}{6}\Big) \\ m(1-\nu)\frac{Rh^3}{6} & c_{22} & c_{23} & -m(2\mu-3\nu)\frac{Rh^3}{12} \\ -\nu Rh & c_{32} & c_{33} & m^2\mu\frac{Rh^3}{12}-\nu Rh \\ -\nu\Big(R^2h+\frac{h^3}{6}\Big) & -m(2\mu-3\nu)\frac{Rh^3}{12} & m^2\mu\frac{Rh^3}{12}-\nu Rh & c_{44} \end{vmatrix} = 0 \tag{4.7}$$

where

$$
\begin{aligned}
c_{11} &= (1-\nu)\Big(R^2h + \frac{h^3}{12}\Big)\\
c_{22} &= m^2(1-\nu)\Big(\frac{R^2h^3}{12} + \frac{h^5}{80}\Big) - \mu\Big(R^2h + \frac{h^3}{12}\Big)\\
c_{23} &= -c_{32} = -m\mu\Big(R^2h + \frac{h^3}{12}\Big) + m\nu\frac{h^3}{12}\\
c_{33} &= m^2\mu\Big(R^2h + \frac{h^3}{12}\Big) - (1-\nu)h\\
c_{44} &= m^2\mu\Big(\frac{R^2h^3}{12} + \frac{h^5}{80}\Big) - (1-\nu)R^2h - \frac{h^3}{6}
\end{aligned}
$$

Similarly, with solving of thr obtained polynomials of Eq. (4.7), the eigenvalues m_i and the following eigenvectors $\mathbf{V}_i$ are calculated, and then, rhe total solution (Eq. (3.9)), with using boundary conditions is obtained.

Based on PET in the plane strain state, the radial stress, circumferential stress, axial stress, and radial displacement are as follows (Ghannad *et al.*, 2010)

$$
\begin{aligned}
\sigma_r &= \frac{P(\overline{r})^{n-1}}{k^{m_1} - k^{m_2}}(k^{m_2}\,\overline{r}^{m_1} - k^{m_1}\,\overline{r}^{m_2})\\
\sigma_\theta &= \frac{P(\overline{r})^{n-1}}{k^{m_1} - k^{m_2}}\Big[\frac{1-\nu+\nu m_1}{(1-\nu)m_1+\nu}k^{m_2}\,\overline{r}^{m_1} - \frac{1-\nu+\nu m_2}{(1-\nu)m_2+\nu}k^{m_1}\,\overline{r}^{m_2}\Big]\\
\sigma_x &= \nu(\sigma_r + \sigma_\theta)
\end{aligned}
\tag{4.8}
$$

and

$$
u_r = \frac{P(r_i)(1+\nu)(1-2\nu)}{E_i(k^{m_1} - k^{m_2})}\Big[\frac{1}{(1-\nu)m_1+\nu}k^{m_2}\,\overline{r}^{m_1} - \frac{1}{(1-\nu)m_2+\nu}k^{m_1}\,\overline{r}^{m_2}\Big] \tag{4.9}
$$

where $\overline{r} = r/r_i$ and $k = r_o/r_i$.

5. Results and discussion

In this section, we present the results for a nonhomogeneous and isotropic clamped-clamped thick hollow cylindrical shell with $r_i = 40\,\text{mm}$, $R = 50\,\text{mm}$, $h = 20\,\text{mm}$ and $L = 800\,\text{mm}$ for $n = +1$, $n = 0$ (Ghannad and Nejad, 2010), and $n = -1$. The modulus of elasticity at the internal radius and Poisson's ratio have values of $E_i = 200\,\text{GPa}$ and $\nu = 0.3$, respectively. The applied internal pressure is $80\,\text{MPa}$. The shear correction factor $K = 5/6$ is considered (Vlachoutsis, 1992; Jemielita, 2002). The analytical solution is carried out by writing a program in MAPLE 13. The numerical solution is obtained through the finite element method (FEM).

The distribution of radial displacement at different layers for $n = +1$ is plotted in Fig. 2. The radial displacement at points away from the boundaries depends on the radius whereas at points near boundary, the radial displacement depends on the radius and length. Figure 3 shows the distribution of axial displacement for $n = +1$ at different layers. At points away from the boundaries, the axial displacement does not show significant differences in different layers, while at points near the boundaries, the reverse holds true. The distribution of circumferential stress in different layers for $n = +1$ is shown in Fig. 4. In the same layer, at points away from the boundaries, the circumferential stress depends on the radius whereas at points near boundary,

the circumferential stress depends on the radius and length. The circumferential stress at layers close to the external surface at points near the boundary is negative, and at other layers positive.

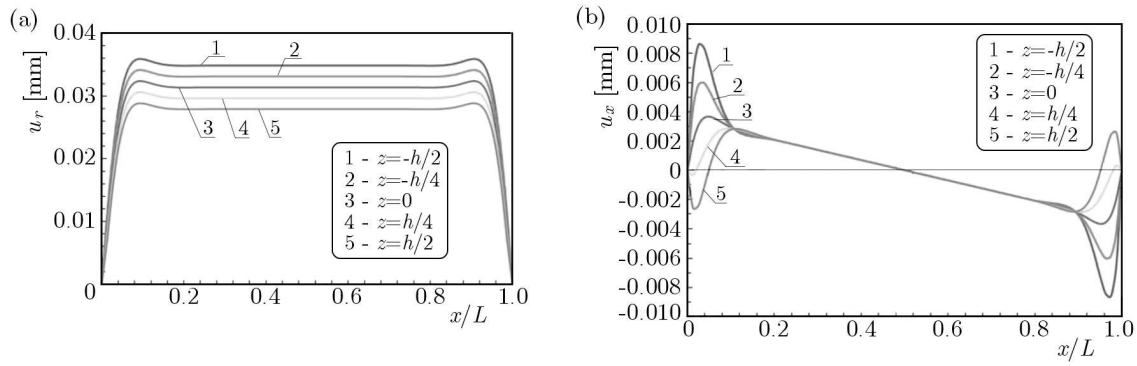

Fig. 2. Radial (a) and axial (b) displacement distribution in different layers $(n = +1)$

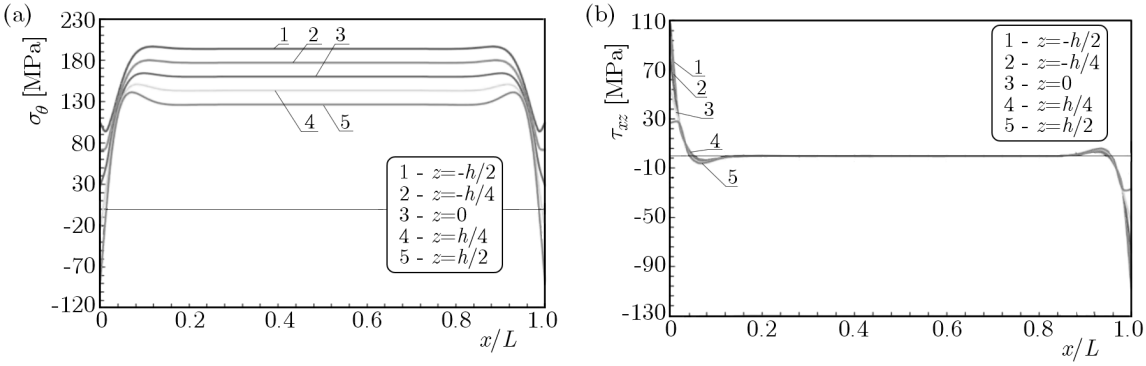

Fig. 3. Circumferential (a) and shear (b) stress distribution in different layers $(n = +1)$

According to Figs. 2 and 3, the greatest axial and radial displacements, circumferential and shear stresses occur in the internal surface. The distribution of shear stress at different layers is shown in Fig. 3b. The shear stress at points away from the boundaries at different layers is the same and trivial. However, at points near the boundaries, the shear stress is significant, especially in the internal surface, which is the greatest. The distribution of radial displacement of the cylinder for different values of n in the middle layer is shown in Fig. 4a. It is observed that the radial displacement depends on the material inhomogeneity constant and there is a decrease in the value of the radial displacement as n increases. The distribution of axial displacement of the cylinder for different values of n in the middle layer is shown in Fig. 4b. As the value of n increases, the axial displacement decreases. The radial stress distribution for different values of n in the middle layer of the cylinder is shown in Fig. 5a. According to this figure, changes in the inhomogeneity constant do not have a significant effect on the radial stress, and the shear stress at points away from the boundaries at different layers is the same. The distribution of axial stress of the cylinder for different values of n in the middle layer is shown in Fig. 5b. It is observed that the axial stress depends on the material inhomogeneity constant. The distribution of circumferential stress of the cylinder for different values of n in the middle layer is shown in Fig. 10. According to this figure, at points near boundaries, changes in the inhomogeneity constant do not have a significant influence on the circumferential stress. It is seen from Fig. 6a that at points away from the boundaries for higher values of n, the circumferential stress increase. Figure 11 shows the distribution of shear stress for different values of n along the middle layer. The shear stress at points away from the boundaries for different values of n is the same and trivial. However, at points near the boundaries, the stress is significant.

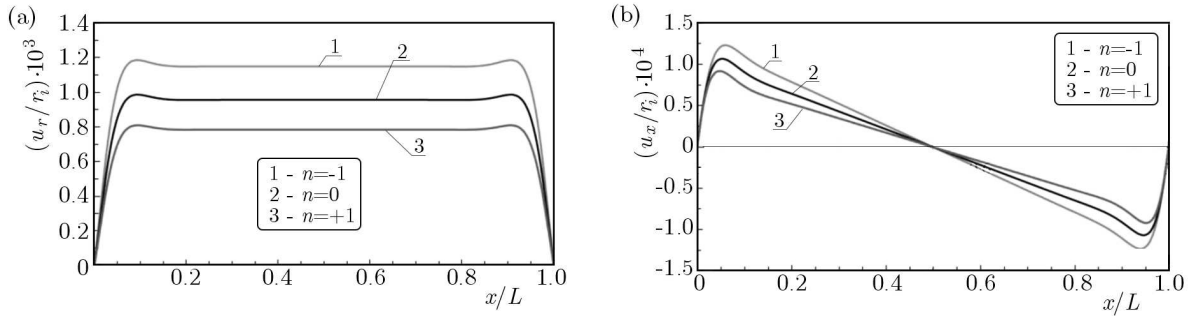

Fig. 4. Radial (a) and axial (b) displacement distribution in the middle surface

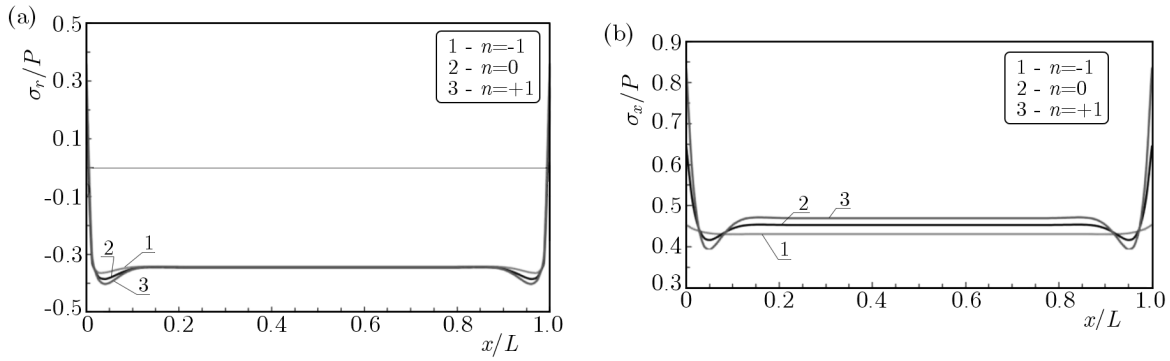

Fig. 5. Radial (a) and axial (b) stress distribution in the middle surface

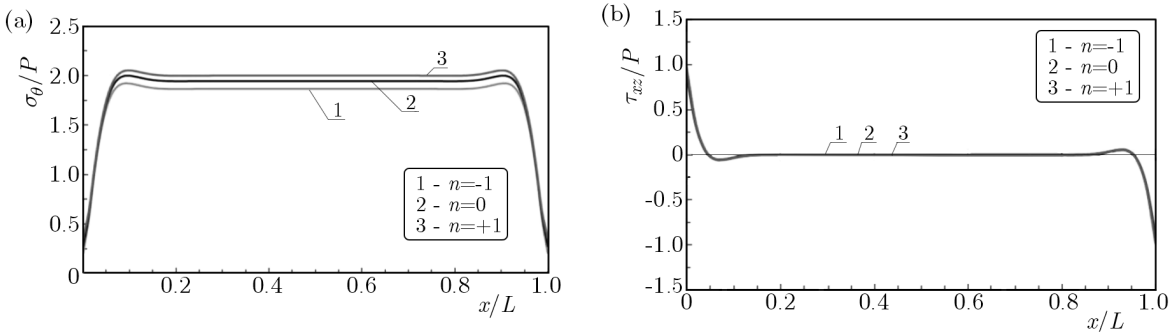

Fig. 6. Circumferential (a) and shear (b) stress distribution in the middle surface

Table 1 presents the results of different solutions for the middle of the FGM cylinder ($x = L/2$) and the middle surface ($z = 0$). The results suggest that in points further away from the boundary it is possible to make use of PET.

Table 1. Numerical data from FSDT, FEM, and PET calculations for $n = -1$ and $n = +1$ in $x = L/2$ and $z = 0$

	$n = -1$				$n = +1$			
	σ_r [MPa]	σ_θ [MPa]	σ_x [MPa]	u_r [mm]	σ_r [MPa]	σ_θ [MPa]	σ_x [MPa]	u_r [mm]
FSDT	−27.34	149.3	34.49	0.04600	−27.52	160	37.57	0.03140
FEM	−24.79	152.61	35.78	0.04570	−31.64	157.36	36.05	0.03188
PET	−24.82	151.08	37.88	0.04600	−31.61	159.12	38.25	0.03143

6. Conclusions

In the present study, the advantages as well as the disadvantages of the PET (Lamé solution) for hollow thick-walled cylindrical shells were indicated. Regarding the problems which could not be solved through PET, the solution based on the FSDT is suggested. At the boundary areas of a thick-walled cylinder with clamped-clamped or clamped-free ends, having constant thickness and uniform pressure, given that displacements and stresses are dependent on radius and length, use cannot be made of PET, and FSDT must be used. In the areas further away from the boundaries, as the displacements and stresses along the cylinder remain constant and dependent on radius, PET ought to be used. The shear stress in boundary areas cannot be ignored, but in areas further away from the boundaries, it can be ignored. Therefore, the PET can be used, provided that the shear strain is zero. The maximum displacements and stresses in all the areas of the cylinder occur on the internal surface. The analytical solutions and the solutions carried out through the FEM show good agreement.

References

1. Batra R.C., Nie G.J., 2010, Analytical solutions for functionally graded incompressible eccentric and non-axisymmetrically loaded circular cylinders, *Composite Structures*, **92**, 1229-1245
2. Eipakchi H.R., Rahimi G.H., Khadem S.E., 2003, Closed form solution for displacements of thick cylinders with varying thickness subjected to nonuniform internal pressure, *Structural Engineering and Mechanics*, **16**, 6, 731-748
3. Ghannad M., Nejad M.Z., 2010, Elastic analysis of pressurized thick hollow cylindrical shells with clamped-clamped ends, *Mechanika*, **85**, 5, 11-18
4. Ghannad M., Rahimi G.H., Khadem S.E., 2010, General plane elasticity solution of axisymmetric functionally graded cylindrical shells, *Journal of Modares Technology and Engineering*, **10**, 3, 31-43 [in Farsi]
5. Ghannad M., Rahimi G.H., Nejad M.Z., 2012, Determination of displacements and stresses in pressurized thick cylindrical shells with variable thickness using perturbation technique, *Mechanika*, **18**, 1, 14-21
6. Hongjun X., Zhifei S., Taotao Z., 2006, Elastic analyses of heterogeneous hollow cylinders, *Mechanics Research Communications*, **33**, 5, 681-691
7. Jemielita G., 2002, Coefficients of shear correction in transversely nonhomogeneous moderately thick plates, *Journal of Theoretical and Applied Mechanics*, **40**, 1, 73-84
8. Kang J.H., 2007, Field equations, equations of motion, and energy functionals for thick shells of revolution with arbitrary curvature and variable thickness from a three-dimensional theory, *Acta Mechanica*, **188**, 1/2, 21-37
9. Mirsky I., Hermann G., 1958, Axially motions of thick cylindrical shells, *Journal of Applied Mechanics, Transactions of the ASME*, **25**, 97-102
10. Naghdi P.M., Cooper R.M., 1956, Propagation of elastic waves in cylindrical shells, including the effects of transverse shear and rotary inertia, *Journal of the Acoustical Society of America*, **29**, 1, 56-63
11. Nejad M.Z., Rahimi G.H., 2010, Elastic analysis of FGM rotating cylindrical pressure vessels, *Journal of the Chinese Institute of Engineers*, **33**, 4, 525-530
12. Nejad M.Z., Rahimi G.H., Ghannad M., 2009, Set of field equations for thick shell of revolution made of functionally graded materials in curvilinear coordinate system, *Mechanika*, **77**, 3, 18-26
13. Nie G.J., Batra R.C., 2010, Material tailoring and analysis of functionally graded isotropic and incompressible linear elastic hollow cylinders, *Composite Structures*, **92**, 265-274

14. Ostrowski P., Michalak B., 2011, Non-stationary heat transfer in a hollow cylinder with functionally graded material properties, *Journal of Theoretical and Applied Mechanics*, **49**, 2, 385-397

15. Pan E., Roy A.K., 2006, A simple plane-strain solution for functionally graded multilayered isotropic cylinders, *Structural Engineering and Mechanics*, **24**, 727-740

16. Suzuki K., Konnon M., Takahashi S., 1981, Axisymmetric vibration of a cylindrical shell with variable thickness, *Bulletin of the JSME*, **24**, 198, 2122-2132

17. Tutuncu N., Temel B., 2009, A novel approach to stress analysis of pressurized FGM cylinders, disks and spheres, *Composite Structures*, **91**, 385-390

18. Vlachoutsis S., 1992, Shear correction factors for plates and shells, *International Journal for Numerical Methods in Engineering*, **33**, 7, 1537-1552

19. Zhifei S., Taotao Z., Hongjun X., 2007, Exact solutions of heterogeneous elastic hollow cylinders, *Composite Structures*, **79**, 1, 140-147

Manuscript received December 24, 2011; accepted for print June 25, 2013